*J. Fluid Mech.* (1964), *vol.* 20, *part* 2, *pp.* 337–352
*Printed in Great Britain*



# An experimental investigation of the instability of a two-dimensional jet at low Reynolds numbers

By HIROSHI SATO AND FUJIHIKO SAKAO
Institute of Space and Aeronautical Science, University of Tokyo, Meguro-ku, Tokyo, Japan

(Received 11 March 1964)

An experimental investigation was made of the stability of a two-dimensional jet at low Reynolds numbers with extremely small residual disturbances both in and around the jet. The velocity distribution of a laminar jet is in agreement with Bickley's theoretical result. The stability and transition of a laminar jet are characterized by the Reynolds number based on the slit width and the maximum velocity of the jet. When the Reynolds number is less than 10, the whole jet is laminar. When the Reynolds number is between 10 and around 50, periodic velocity fluctuations are found in the jet. They die out as they travel downstream without developing into irregular fluctuations. When the Reynolds number exceeds about 50, periodic fluctuations develop into irregular, turbulent fluctuations. The frequency of the periodic fluctuation is roughly proportional to the square of the jet velocity.

The stability of the jet against an artificially imposed disturbance was also investigated. Sound was used as an artificial disturbance. The disturbance is either amplified or damped in the jet depending on its frequency. The conventional stability theory was modified by considering the streamwise increase of Reynolds number. The experimental results are in agreement with the theoretical results.

## 1. Introduction

One of the most important features of free shear-layers such as wakes and jets is that they are extremely unstable. A theoretical investigation of the stability of a two-dimensional jet was made by Savic (1941) when the Reynolds number is very large. Stability calculations at low Reynolds numbers were made by Curle (1957), Howard (1958), Tatsumi & Kakutani (1958) and Clenshaw & Elliott (1960). The critical Reynolds number of instability is estimated to be less than 10. These stability calculations are based on the Orr–Sommerfeld equation which is essentially a linearized equation of motion for small perturbations superposed on the basic flow.

Early experiments on a jet were mainly concerned with the generation of sound from the jet (Kohlrausch 1881; Kruger & Schmidtke 1919; Brown 1935) and were conducted at considerably higher Reynolds numbers. In 1939 Andrade made a measurement on the velocity distribution of a two-dimensional water-to-water jet at low Reynolds numbers and found a good agreement with the theoretical results of Bickley (1937). Andrade observed that the jet becomes unstable when the Reynolds number based on the effusion velocity and the width

of the slit exceeds about 10. His experimental results on the instability were insufficient for making a quantitative discussion on the stability characteristics at low Reynolds numbers. Recently, Chanaud & Powell (1962) observed the stability of a two-dimensional water-to-water jet in the range of Reynolds number from several tens to 400. They measured also the velocity distribution of a low Reynolds number air jet. Their results on the stability showed a qualitative agreement with theoretical predictions.

One of the authors (Sato 1960) carried out a detailed investigation of the instability and transition of a two-dimensional jet at high Reynolds numbers. He has shown that observed values of the amplification rate, the propagation velocity and the amplitude distribution of small-amplitude velocity fluctuations are in good agreement with the theoretical results based on the Orr–Sommerfeld equation. The present experiment, as a direct extension of the previous work, was made with the intention of observing the instability of a two-dimensional jet at extremely low Reynolds numbers. The experimental results were compared with the theoretical results. The transition process from a laminar to a turbulent jet was also observed.

## 2. Experimental arrangement

Two rectangular nozzles with different slit sizes were used for producing two-dimensional jets of various Reynolds numbers. Slits were 0·2 mm by 30 mm and 1·1 mm by 100 mm. Aspect ratios of the two nozzle slits were 150 and 90, respectively. Detailed measurements were made by using the smaller nozzle. The range of the jet velocity at the centre of the nozzle slit was from 90 to 1500 cm/s and the Reynolds number at the slit $R_s = 2U_{00}h/\nu$ ($U_{00}$ being the velocity at the centre of the nozzle slit, $2h$ the width of the slit and $\nu$ the kinematic viscosity) varied from 12 to 200 with the smaller nozzle and from 320 to 1200 with the larger nozzle.

Details of the test section are illustrated in figure 1. Air is supplied from an air tank, into which water is introduced from a small hole. The air in the tank is replaced by the water and comes out of the top of the tank. The flow of air is controlled by a water valve. This system is free from the sound noise and mechanical vibrations which have fatal effects on the stability of a jet. The air from the tank goes through a settling chamber and is accelerated by a two-dimensional contraction. To the contraction is connected a parallel channel which has the same cross-section as the nozzle slit and is long enough for realizing a parabolic velocity distribution at the nozzle exit. The air issuing from the nozzle induces an air flow from both sides of the jet. In order to reduce the disturbance introduced into the induced flow a faired passage was provided as shown in the figure. The test-section was surrounded by two pairs of walls. One is shown in the figure and the other pair of walls is attached to both ends of the nozzle slit for consolidating the two-dimensionality of the jet. Experiments were carried out in an isolated silent room free from draught, sound noise and mechanical vibrations.

A hot-wire anemometer was used exclusively for measuring mean and fluctuating velocities. The hot-wire was inserted through a rectangular hole in one of the walls shown in figure 1 and moved in $X$- (parallel to the jet) and $Y$-directions

(perpendicular to the jet and the slit) with precision micrometers. The calibration of the hot-wire was made by placing it on the axis of a long circular pipe which was made especially for the calibration. The air was supplied to the pipe from the same air tank. Since the volume flow of air is known and the velocity distribution at the exit of the pipe is expected to be parabolic, the velocity on the axis is determined. By using this procedure for calibration, the flow velocity down to

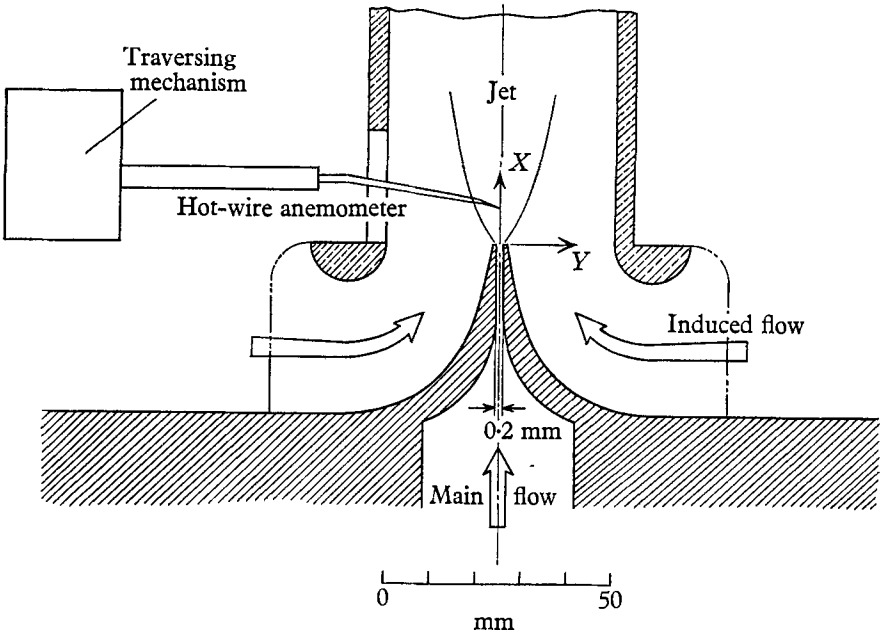


FIGURE 1. Experimental set-up.

20 cm/s was measured with considerable accuracy. The volume flow of air at the slit calculated from the hot-wire measurement showed good agreement with the volume flow of water into the tank. The hot-wire anemometer was operated by a constant current method and the voltage output from the wire was amplified either by an a.c. amplifier with an appropriate high-frequency compensation or by a d.c. amplifier without compensation depending on the frequency of fluctuations. The frequency range of the velocity fluctuations was approximately from 2 to 1000 c/s. The output of the amplifier was fed to a cathode-ray oscilloscope. The wave-form of the velocity fluctuation was recorded by taking pictures of the screen of the oscilloscope.

The jet was excited by an artificial disturbance when necessary. A 10 W loudspeaker was used for this purpose. The maximum available intensity of the sound from the loudspeaker was 80 decibels at the nozzle exit.

## 3. Mean-velocity distribution

Experiments were carried out in three steps. First, measurements were made of the distribution of the time-mean velocity. Secondly, the velocity fluctuation in the natural transition was observed. Thirdly, the instability of the jet due to

artificial disturbances was investigated. Figure 2 shows the mean-velocity distribution which was measured by a hot-wire anemometer with the velocity at the centre of the slit $U_{00} = 313$ cm/s. The slit Reynolds number is 42. The velocity on the centre-line of the jet decreases and the width of the jet increases downstream. The distribution itself seems to be similar at various $X$-stations. This similarity is clearly demonstrated in figure 3 in which $U$ is normalized by the

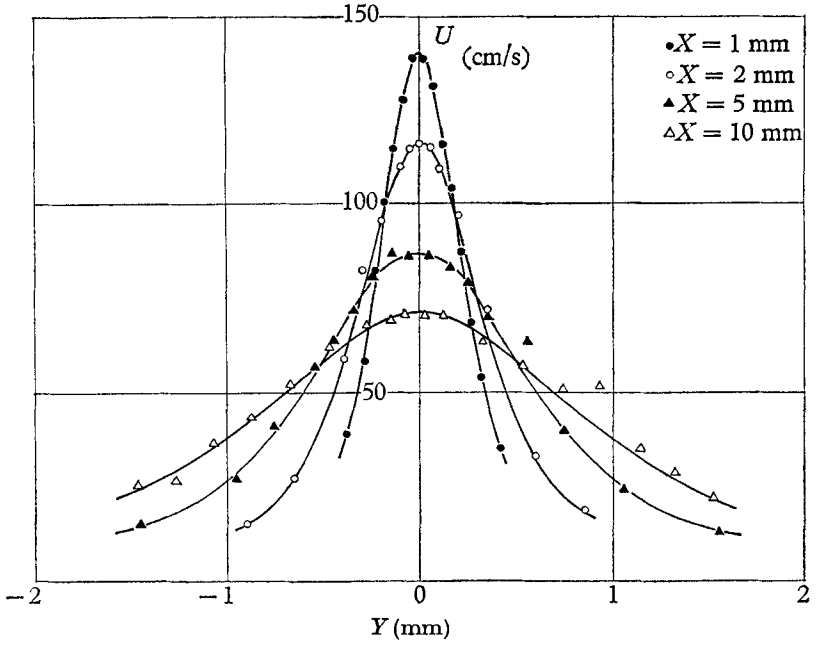


FIGURE 2. Lateral distribution of time-mean velocity. Slit 0·2 mm. Velocity at the centre of the slit, 313 cm/s.

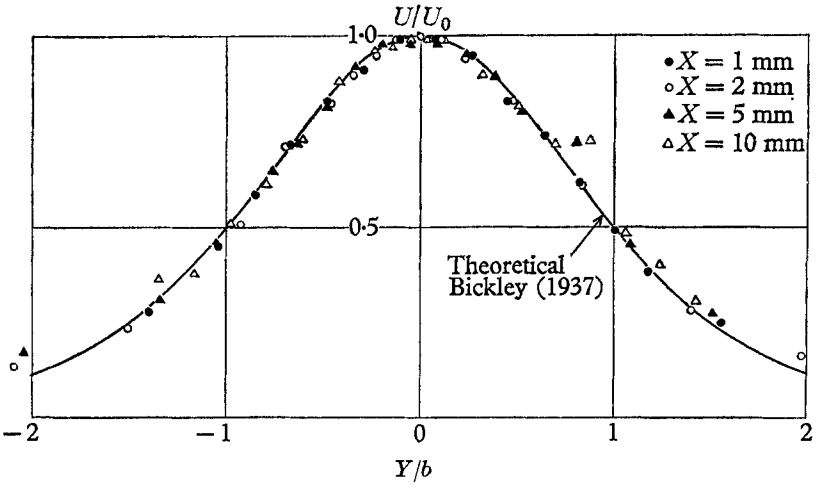


FIGURE 3. Non-dimensionalized distribution of mean velocity. Slit 0·2 mm. Solid line is the theoretical distribution given by Bickley (1937).

maximum speed $U_0$ at each $X$-station and $Y$ is non-dimensionalized by the half breadth $b$—the distance from the centre line to the point where $U/U_0 = \frac{1}{2}$.

Bickley (1937) calculated the velocity distribution of a laminar two-dimensional jet and gave an analytical expression,

$$U/U_0 = \operatorname{sech}^2 aY/b \quad (a = 0{\cdot}88136).$$

In figure 3 the theoretical curve (solid line) is compared with experimental results. The agreement between the theoretical and experimental results is fairly good. Bickley's calculation gives the variations of $U_0$ and $b$ in the flow direction

$$U_0 = \left(\frac{3M^2}{32\nu X}\right)^{\frac{1}{3}}, \quad b = a\left(\frac{48\nu^2X^2}{M}\right)^{\frac{1}{3}},$$

in which $M$ is defined as

$$M = \int_{-\infty}^{\infty} U^2 dY.$$

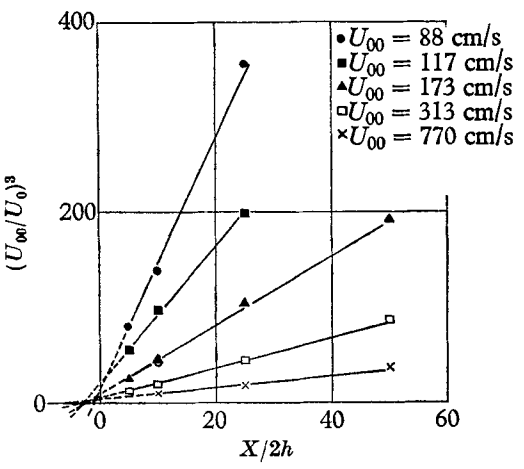


FIGURE 4. Streamwise variation of central velocity. Slit 0·2 mm.

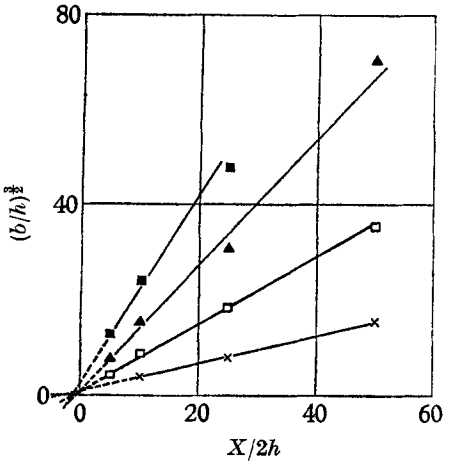


FIGURE 5. Streamwise variation of the half breadth of the jet. Slit 0·2 mm.

Considering that no external force is present in the flow field the momentum of the jet must be constant. Therefore, $U_0^{-3}$ and $b^{\frac{3}{2}}$ are considered to be proportional to $X$. Experimental results on $U_0$ and $b$ are plotted in figures 4 and 5. Both $(U_{00}/U_0)^3$ and $(b/h)^{\frac{3}{2}}$ are linear to $X/2h$. In other words, $M$ is shown to be constant throughout the flow field. However, each line starts from a virtual origin which is different from the geometrical origin. This is because the nozzle slit has a finite width and moreover the velocity distribution at the slit is not of jet-type distribution but parabolic. A self-similar velocity distribution is established at some distance downstream. These results are close to the results of Andrade (1939) which were obtained in a water-to-water jet.

The location of the virtual origin is determined by the extrapolation of $U_0^{-3}$ *vs* $X$ curve and plotted against the slit Reynolds number in figure 6. The virtual origin seems to move upstream as the Reynolds number increases. Data obtained by Andrade and Chanaud & Powell are also plotted. There is a discrepancy between

the data of the different investigators. The discrepancy might come primarily from the difference in the nozzle geometry.

The kinematic momentum $M$ calculated from the gradient of the $U_0^{-3}$ *vs* $X$ curve is shown in figure 7. Values of $M$ thus obtained are considerably less than the value at the nozzle exit calculated from

$$M_0 = \int_{-h}^{h} U^2 dY.$$

The ratio $M/M_0$ lies between 0·5 and 0·8. Calculated values from the data of Chanaud & Powell are also shown. No detailed mechanism of loss of momentum is known. One of the authors (Sato 1960) found that there is a low-pressure region

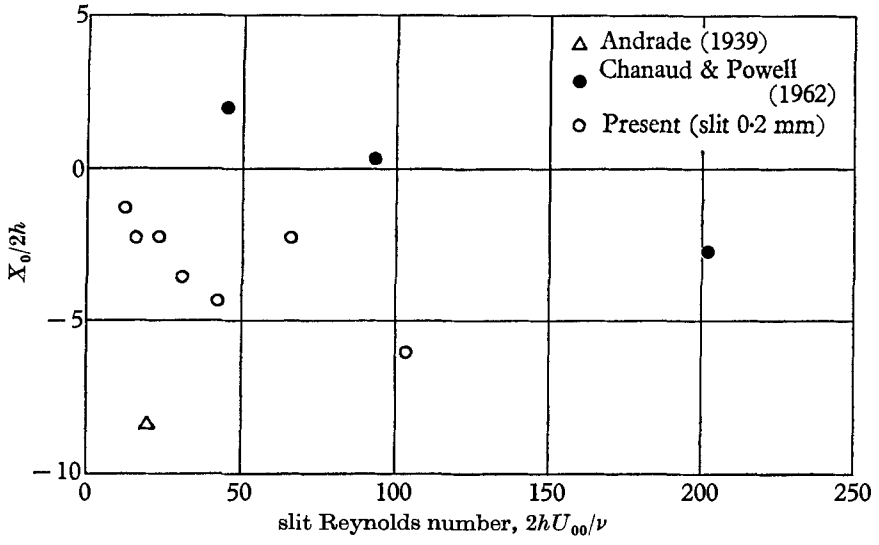


FIGURE 6. Location of virtual origin *vs* slit Reynolds number. $X_0$ denotes the location of the virtual origin measured from the slit in the flow direction.

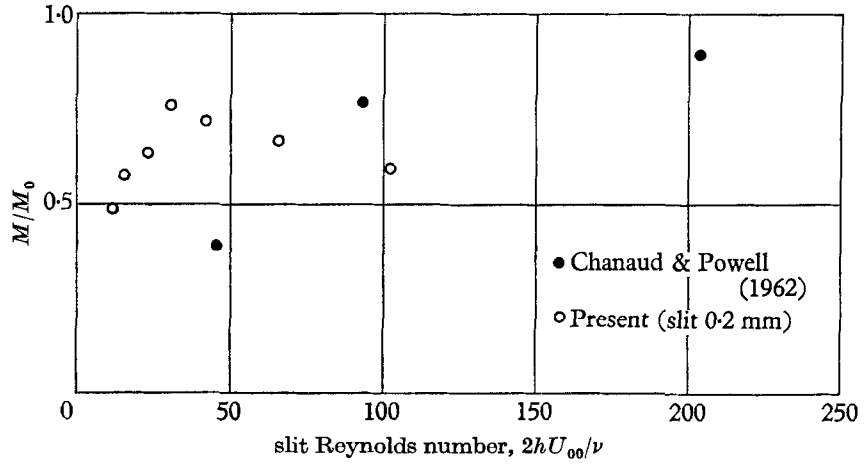


FIGURE 7. Kinematic momentum $M$ of the jet *vs* slit Reynolds number. $M_0$ denotes the kinematic momentum at the slit.

in the jet near the nozzle exit. The loss of momentum might be related to the presence of the low-pressure region.

It is concluded that Bickley's calculation of the mean-velocity distribution is in good agreement with the present experimental results if the location of the origin is properly shifted and the momentum loss is properly taken into account. In comparison with experimental results on a high Reynolds number jet (Sato 1960) it is noticed that at low Reynolds number a laminar jet is established before velocity fluctuations appear. At a high Reynolds number the amplification of disturbances is very rapid and the transition takes place at about $X/2h = 5 \sim 10$ where the mean velocity is still almost parabolic rather than in the form of $\mathrm{sech}^2 Y/b$. The difference of mean-velocity distributions at high and low Reynolds numbers causes a difference in the stability characteristics. A detailed discussion of this point will be made later.

## 4. Velocity fluctuations

When residual disturbances in and around a jet are made extremely small, the transition from a laminar to a turbulent jet is considered to be the 'natural transition'. Even in this case the transition is caused by small and uncontrollable

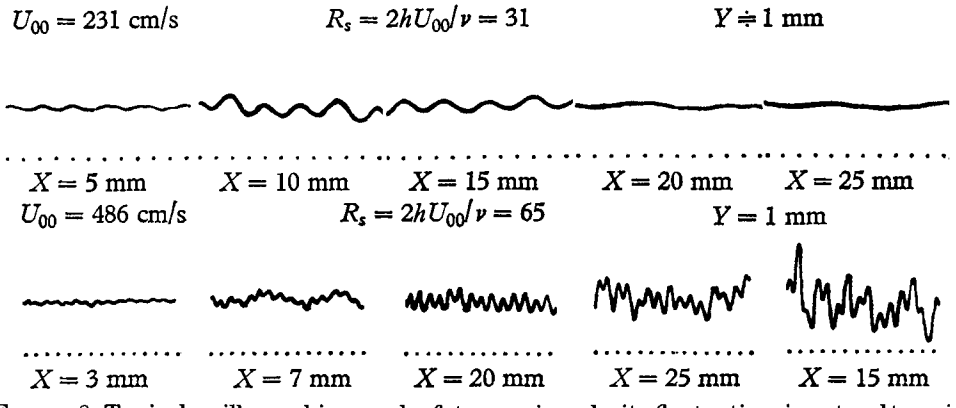


FIGURE 8. Typical oscillographic records of streamwise velocity fluctuations in natural transition. Slit 0·2 mm. Time is from left to right and the intervals between dots are 0·01 s.

disturbances. The intensity of the residual disturbances might be different from one run to another and from day to day. In this sense the definition of 'natural transition' is vague and one is not expected to obtain the same experimental result for each run. Data presented here are results averaged over repeated observations.

A survey of the velocity fluctuation was made by a hot-wire anemometer which is sensible only for the $u$-fluctuation. Some examples of oscillographic records of velocity fluctuations are reproduced in figure 8. At small values of $X$, wave-forms of fluctuations are almost sinusoidal, the higher frequency corresponding to the higher wind-speed. Figure 9 shows a map of streamwise velocity fluctuations obtained from the survey. In hatched regions are found periodic velocity fluctuations. In regions hatched by broken lines the existence of periodic fluctuations is not definite. In regions left blank no $u$-fluctuation is found.

This does not mean that there are no velocity fluctuations in those regions. At the centre of the jet, for example, the lateral velocity fluctuation might have a maximum amplitude. At low Reynolds numbers velocity fluctuations are found only in a very small region (figure 9 (*a*)). The region of sinusoidal fluctuation

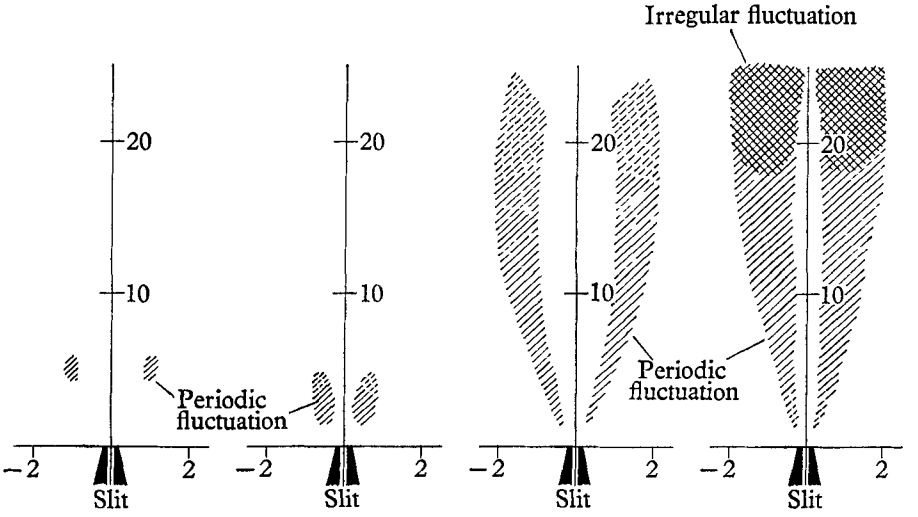


(*a*) $U_{00} = 88$ cm/s $R_s = 2hU_{00}/\nu = 12$ (*b*) $U_{00} = 116$ cm/s $R_s = 16$ (*c*) $U_{00} = 231$ cm/s $R_s = 31$ (*d*) $U_{00} = 486$ cm/s $R_s = 65$

FIGURE 9. Map of patterns of streamwise velocity fluctuations. Slit 0·2 mm, unit in millimetres.

becomes broader as the Reynolds number is increased. An irregular wave-form is not observed anywhere in the jet until the slit Reynolds number reaches 65 (figure 9 (*d*)). The periodic velocity fluctuation at low Reynolds number dies out before the wave-form of the fluctuation becomes irregular. If the irregular wave-form represents a turbulent state, the transition Reynolds number, based on the maximum speed at the slit and on the width of the slit, is around 50.

The reason why some disturbances appear and then disappear again will be discussed in the next section.

The dependence of the frequency of the sinusoidal velocity fluctuation on the jet velocity is shown in figure 10. When a definite frequency is once established, there are no spatial variations in the frequency in $X$- and $Y$-directions. A simple relation between the frequency and the jet velocity can be deduced from a dimensional consideration.

The frequency might be related to a characteristic velocity $U$ and a characteristic length $L$ by

$$f \propto U/L.$$

In a jet, the characteristic velocity is taken to be the velocity on the centre line, $U_0$ and the characteristic length is the breadth of the jet, $b$. When the Reynolds number is high enough, the central velocity and the breadth does not change much in the $X$-direction in the region where the sinusoidal fluctuation is found.

Therefore, the central speed at the slit $U_{00}$ and the slit width $2h$ might be taken as characteristic quantities. Thus, $f \propto U_{00}/2h$.

The frequency in this case is proportional to the jet velocity. This relation was found experimentally in a high Reynolds number jet (Sato 1960). In a low Reynolds number jet, using Bickley's calculation for the mean-velocity distribution, the characteristic quantities are expressed by

$$U_0 \propto M^{\frac{2}{3}}X^{-\frac{1}{3}}\nu^{-\frac{1}{3}} \propto U_{00}^{\frac{4}{3}}h^{\frac{2}{3}}X^{-\frac{1}{3}}\nu^{-\frac{1}{3}},$$

$$b \propto M^{-\frac{1}{3}}X^{\frac{2}{3}}\nu^{\frac{2}{3}} \propto U_{00}^{-\frac{2}{3}}h^{-\frac{1}{3}}X^{\frac{2}{3}}\nu^{\frac{2}{3}},$$

in which the reduction of momentum near the nozzle is neglected. Then

$$f \propto (U_{00}^2/\nu)(h/X).$$

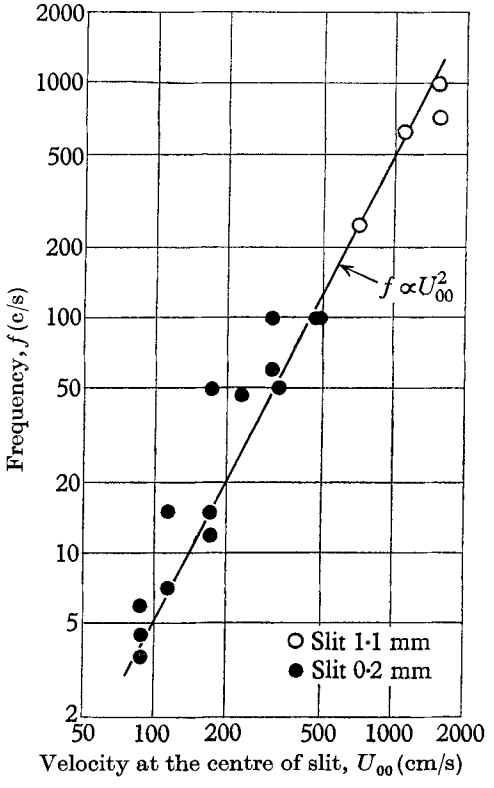


FIGURE 10. Frequency of sinusoidal velocity fluctuations plotted against jet velocity. Solid line shows the relation $f \propto U_{00}^2$.

This means that the frequency is proportional to $U_{00}^2$. This relation is in contrast with that of a high Reynolds number jet. A full straight line in figure 10 illustrates the relation $f \propto U_{00}^2$. Experimental points lie roughly on the straight line regardless of the difference in the slit width.

In figure 11, a non-dimensionalized frequency, $S_j$ ($= 2hf/U_{00}$) is plotted against the slit Reynolds number $2hU_{00}/\nu$. Values of $S_j$ are between $10^{-3}$ and $10^{-2}$ at low Reynolds numbers. At high Reynolds numbers $S_j$ is one order of magnitude larger than the value at low Reynolds numbers. It is interesting to note that the

same tendency is found for the Strouhal number of a wake of a two-dimensional cylinder (Roshko 1954).

As mentioned before, when the slit Reynolds number exceeds about 50, the wave-form of the periodic velocity fluctuation becomes irregular at a large distance from the slit. However, this does not necessarily mean that a fully developed turbulent jet is established. The velocity fluctuation may die out before energy equilibrium is achieved. The periodic wave-form gradually changes into an irregular pattern. No turbulent spots or bursts were observed.

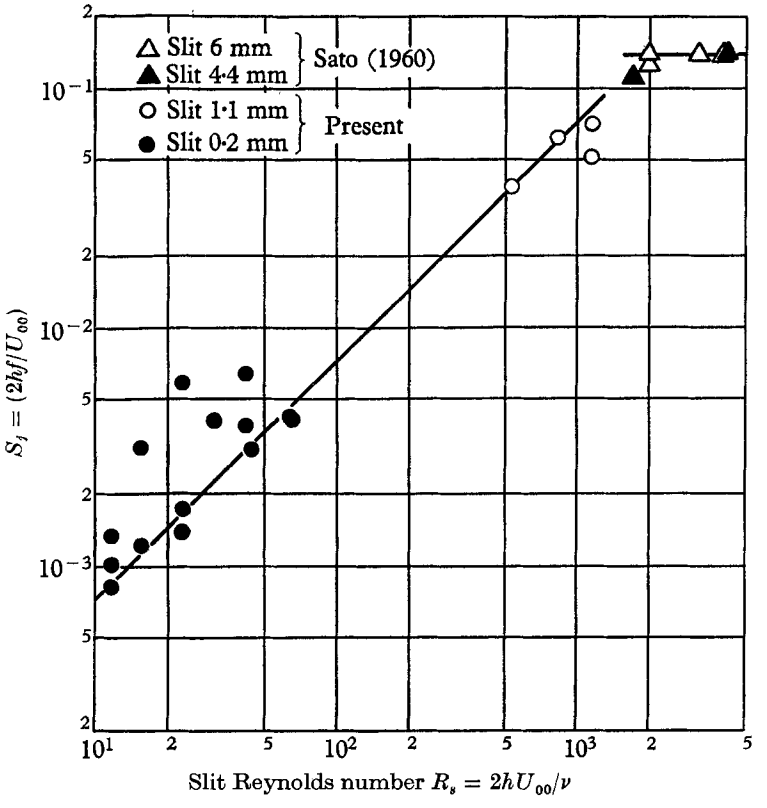


FIGURE 11. Non-dimensionalized frequency of sinusoidal velocity fluctuations plotted against slit Reynolds number.

The instability of a jet due to artificial disturbances was investigated by introducing sound into the jet from a loudspeaker placed near the jet. An audio-frequency oscillator was used for exciting the loudspeaker with a sinusoidal wave-form in the frequency range between 30 and 2000 c/s. Since the wavelength of sound is large compared with the dimensions of the jet, the disturbance is considered to be uniform in the jet. In other words, the whole jet is excited with the same intensity and phase. The difference in the exciting effect due to the relative position of the loudspeaker and the jet was not detected experimentally. The exciting sound must be loud enough to produce noticeable effects in the jet. On the other hand, if the intensity of the sound is too large, an immediate transition to a turbulent jet or a non-linear development of the imposed disturbance

takes place. Therefore, the intensity of the sound should not exceed a certain limit. Considering these facts, the intensity of the sound was made to be about 60 decibels at the jet.

Effects of sound on the instability of a jet are different for different frequencies. The effect is detected by comparing outputs of a hot-wire anemometer in the absence and in the presence of sound. If the output increases in the presence of sound, the disturbance is registered as 'amplified'. If the sound makes no

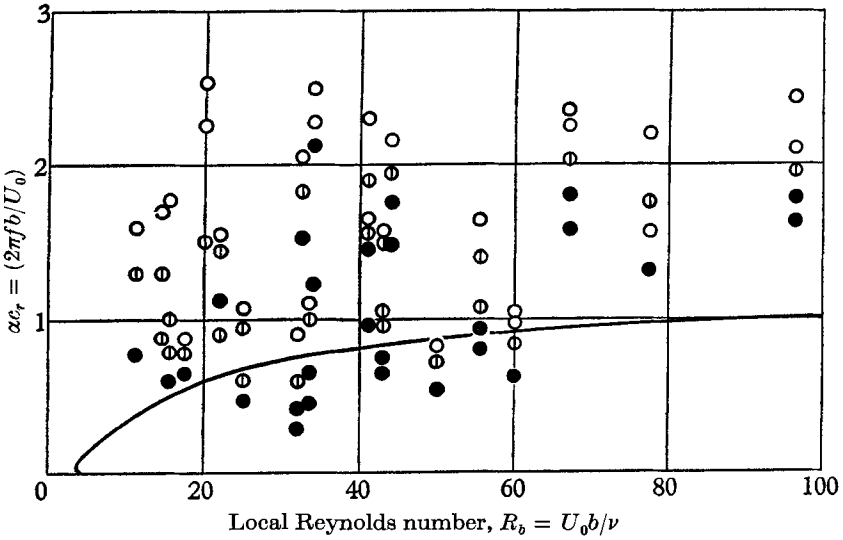


FIGURE 12. Amplification and damping of fluctuations induced by sound. Slit 0·2 mm. ●, Amplified; ○, not amplified; ⊕, not clear. Ordinate: frequency of fluctuation non-dimensionalized by local flow conditions $U_0$ and $b$. Abscissa: local Reynolds number $R_b = U_0 b/\nu$. Solid line shows the theoretical neutral stability curve given by Tatsumi & Kakutani (1958).

difference in the output the disturbance is registered as 'not amplified'. The experimental results are shown in figure 12. The ordinate and abscissa are the non-dimensional frequency and the Reynolds number, respectively, both based on the central speed $U_0$ and the half breadth $b$. The full line in the figure is the theoretical neutral curve calculated by Tatsumi & Kakutani (1958). Since the fluctuation induced by the sound grows in the flow direction, the observed effect of sound at a certain point in the jet is actually an integrated effect from the nozzle to the point of observation. The comparison of experimental results with the stability theory will be made in the next section.

The wavelength of the induced velocity fluctuation was obtained by measuring the phase relation in the $X$-direction. The wavelength is around 3 to 20 times the half breadth of the jet $b$ depending on the frequency. The propagation velocity calculated from the frequency and the wavelength lies between 0·35 and 0·7 times the central velocity increasing slightly as the Reynolds number increases.

The amplitude distribution of $u$-fluctuation is shown in figure 13. The distribution has a minimum on the centre-line and two peaks on both sides of the jet. The measurement of the phase relation in the $Y$-direction reveals that the phase difference of the artificially induced velocity fluctuation at any two symmetrical

points with respect to the centre-line is approximately 180 degrees. In other words, the induced fluctuation is antisymmetric. This fact indicates that the jet is more unstable for antisymmetric disturbances than for symmetric disturbances.

## 5. Comparison of experimental results with stability theory

In existing stability theories the change of the basic flow in the flow direction is neglected. The perturbation stream function is given in the form

$$\psi(x, y, t) = \phi(y)\, e^{i\alpha(x-ct)},$$

in which $\phi$ is the amplitude function, $\alpha$ the wave-number, $c = c_r + ic_i$, $c_r$ being the propagation velocity and $c_i$ giving the amplification rate. When the Navier–

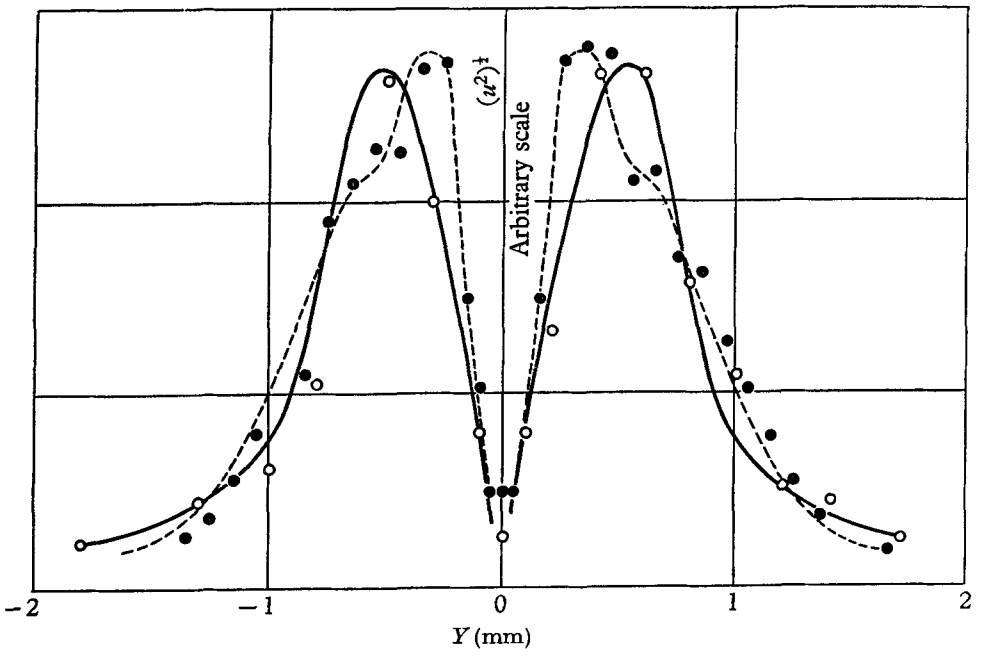


FIGURE 13. Amplitude distributions of velocity fluctuations induced by sound. Slit 0·2 mm. Frequency of sound, 64 c/s. ●, $U_{00} = 173$ cm/s; $X = 2$ mm, $b = 0{\cdot}62$ mm, $R_b = U_0 b/\nu = 20$. ○, $U_{00} = 313$ cm/s; $X = 5$ mm, $b = 0{\cdot}70$ mm, $R_b = 41$.

Stokes equation is linearized by assuming the perturbation is small, the Orr–Sommerfeld equation follows. All quantities in the equation are non-dimensionalized by the central velocity and the width of the jet. As shown before, the central velocity and the jet width change in the flow direction as $X^{-\frac{1}{2}}$ and $X^{\frac{1}{2}}$, respectively. The flow Reynolds number consequently increases downstream as $X^{\frac{1}{2}}$. The applicability of the Orr–Sommerfeld equation at low Reynolds numbers should be determined by estimating the order of magnitude of neglected terms in the equation. The neglected terms are the lateral velocity $V$, and streamwise derivatives such as $\partial U/\partial X$, $\partial^2 U/\partial X^2$. These quantities are estimated by using the Bickley-type velocity distribution.

The maximum value of $V/U$ is given by

$$(V/U)_{\max} = 0{\cdot}795/R_b,$$

in which $R_b = U_0 b/\nu$.

The ratio of maximum values of $\partial U/\partial X$ and $\partial U/\partial Y$ is given by

$$(\partial U/\partial X)_{\max}/(\partial U/\partial Y)_{\max} = 9{\cdot}17/R_b.$$

The ratio of maximum values of $\partial^2 U/\partial X^2$ and $\partial^2 U/\partial Y^2$ is given by

$$(\partial^2 U/\partial X^2)_{\max}/(\partial^2 U/\partial Y^2)_{\max} = -6{\cdot}21/R_b^2.$$

From these results it is obvious that neglecting $V$, $\partial U/\partial X$ and $\partial^2 U/\partial X^2$ is justified at high Reynolds numbers. But at low Reynolds numbers, this gives a considerable error. For instance, for the flow Reynolds number $R_b = 3{\cdot}5$ (which is the theoretical critical Reynolds number, based on the half breadth of a jet, given by Tatsumi & Kakutani for a two-dimensional jet) the values of the three ratios are 0·2, 2·5 and $-0{\cdot}5$, respectively. To neglect the streamwise variation in the stability calculation is not considered valid at such a low Reynolds number.

A difficulty in comparing experimental results with the stability theory comes out of the fact that the frequency, the wavelength and the amplification rate of a disturbance are non-dimensionalized by characteristic quantities, such as the central velocity and the breadth of the jet. When the Reynolds number is small they change considerably in the flow direction. If a disturbance of certain frequency is imposed at some point in a jet, the non-dimensionalized frequency changes in the flow direction as the disturbance travels downstream. If Bickley's velocity distribution is used for the calculation, the non-dimensionalized frequency $\alpha c_r$ changes in proportion to $X$. Since the flow Reynolds number $R_b$ is proportional to $X^{\frac{1}{3}}$, $\alpha c_r$ is proportional to $R_b^3$. The amplification of a superposed disturbance is the integral effect along lines of $\alpha c_r \propto R_b^3$ in the $(\alpha c_r, R_b)$ plane. Thus the spatial amplification $A$ is given by

$$A = \exp\left\{\int_{R_{b0}}^{R_b} 0{\cdot}644(\alpha c_i/c_r)\, dR_b\right\},$$

in which $\alpha c_i/c_r$ is the spatial amplification factor of a small disturbance when the disturbance is considered to be amplified in the $X$-direction instead of along the time axis. There are no positive reasons why the phase velocity $c_r$ is to be used for the transformation between the time-wise and spatial amplification rates. The group velocity may also be used. In the present case the group velocity obtained from the theoretical relation between $\alpha$ and $c_r$ at infinite Reynolds number is about $1{\cdot}6c_r$ in the range $0{\cdot}1 < \alpha c_r < 1{\cdot}15$. The spatial amplification rates calculated by using two velocities are different in the factor of 1·6. The numerical factor 0·644 comes from the proportionality constant between $X$ and $R_b^3$.

In order to execute the integration in the $(\alpha c_r, R_b)$-plane the amplification factor must be known as a function of $\alpha c_r$ and $R_b$. Unfortunately, available theoretical results are either for the case of neutral stability ($c_i = 0$) or for the amplification factor at an infinite Reynolds number. The neutral curve calculated by Tatsumi & Kakutani (1958) was used. The functional form of $\alpha c_i/c_r$ *vs* $\alpha c_r$ was assumed similar to the one at infinite Reynolds number calculated by Lessen & Fox (1955). The starting-point of integration is the flow Reynolds number at the slit.

When the integration is made along a line $\alpha c_r \propto R_b^3$ starting from a point in the unstable zone, $A$ increases at first. At the Reynolds number corresponding to an intersection of the neutral curve and the $\alpha c_r \propto R_b^3$ curve, the value of $c_i$ is zero, and for larger Reynolds numbers $c_i$ is negative. If the integration is made up to the Reynolds number at which $A$ becomes unity, $\alpha c_r$ at that Reynolds number should

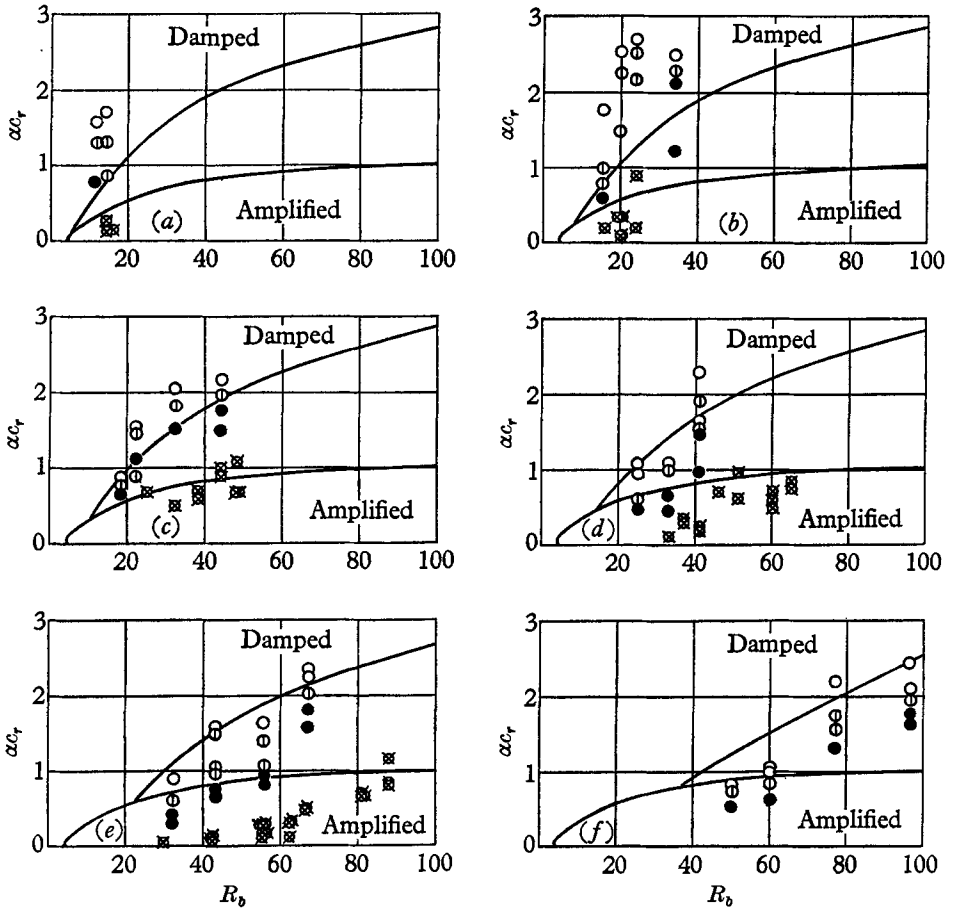


FIGURE 14. Comparison of amplification and damping of fluctuations induced by sound with theory. ●, amplified; ○, not amplified; ⊙, not clear; ⊠, natural fluctuation. (*a*) $U_{00} = 117$ cm/s, $R_s = 16$; (*b*) $U_{00} = 173$ cm/s, $R_s = 23$; (*c*) $U_{00} = 231$ cm/s, $R_s = 31$; (*d*) $U_{00} = 313$ cm/s, $R_s = 42$; (*e*) $U_{00} = 486$ cm/s, $R_s = 65$; (*f*) $U_{00} = 770$ cm/s, $R_s = 103$. Lower branch of solid lines is the neutral stability curve given by Tatsumi & Kakutani (1958). Upper branch is the 'integrated' neutral curve. Circle with cross denotes the frequency of fluctuation observed in natural transition.

give the frequency of the integrated neutral disturbance. In other words, a small disturbance with a definite frequency, starting at the slit is amplified and damped, as it travels downstream, and ends at the same amplitude. By making the integration along various sets of $\alpha c_r \propto R_b^3$ curves, an integrated neutral curve is obtained as shown in figure 14. The use of the group velocity for the transformation gives no difference in the integrated neutral curve because the group velocity is proportional to the phase velocity. It is obvious that for different starting-points,

namely, for different slit Reynolds numbers, different neutral curves are obtained. In figure 14, experimental results are shown with three kinds of symbol for denoting the amplification and damping. Generally speaking, the agreement between the integrated neutral curve and experimental results is good. Crossed circles indicate the frequencies of velocity fluctuations which are found in the natural transition. The frequency lies in the amplified zone. When the Reynolds number is small, that is, $X$ is small, the non-dimensionalized frequency is small. The theoretical maximum amplification is expected to occur at $\alpha c_r$ around 0·2. Experimental values of $\alpha c_r$ at small $R_b$ are not too far from this value.

In the present experiment the Bickley-type velocity distribution is realized before an appreciable growth of a small disturbance occurs. In the previous experiment made at higher Reynolds numbers, on the contrary, the instability takes place in the transient region of the jet, in other words, before the Bickley distribution is established (Sato 1960). These facts are explained by considering the difference in the rates of change for the establishment of the Bickley distribution and for the growth of small disturbances. The distance in which the Bickley distribution is established is roughly the slit width times slit Reynolds number, while the growth rate of disturbances is smaller at smaller Reynolds numbers. Thus at large Reynolds numbers the growth of disturbances is faster than the change of the velocity distribution.

In the natural transition, there are extremely small residual disturbances in and around the jet. They are so small that they are not detected experimentally. Some of the disturbances are amplified in the jet. If the energy of residual disturbances is uniformly distributed over the frequency spectrum, the frequency component which has the maximum amplification rate will dominate the other components. This is the reason why sinusoidal velocity fluctuations are observed in the natural transition. When the Reynolds number is small, the amplification is small. Therefore, the selective amplification due to the difference in the amplification rate is not sharp. This fact explains the observed scatter of frequency of the periodic fluctuation at small Reynolds numbers. These considerations are valid in the region not far from the slit. At a large distance from the slit the jet velocity becomes so small that the velocity fluctuation with an appreciable amplitude does not exist. This is one of the reasons why the velocity fluctuation once observed at small $X$ disappears at large $X$.

The determination of the critical Reynolds number is a fascinating problem in the study of a jet at low Reynolds numbers. This determination is, however, very difficult for the following reasons. In the first place, the basic flow changes in the flow direction and so does the Reynolds number. Secondly, the amplification of a disturbance is small. It is difficult to distinguish the amplification and damping of superposed disturbances. To illustrate this point by a numerical example we consider a small disturbance which is superposed on a jet of Reynolds number 4. The increment of Reynolds number in the flow direction is taken to be 1. The value of the spatial amplification factor $\alpha c_i/c_r$ is assumed to be 0·1 considering that the maximum value at an infinite Reynolds number is 0·3. Then the calculated amplification is 1·06. In order to investigate a linear amplification, the amplitude of the initial disturbance must be very small. The detection of ampli-

fication of 1·06 of such a small disturbance is very difficult. Therefore, the experimental determination of the critical Reynolds number cannot be accurate. The present experimental results give no contradictions to the value of theoretical critical Reynolds number around 4.

## 6. Conclusion

The investigation of stability of a two-dimensional jet at low Reynolds numbers indicated the following conclusions:

(1) The observed mean-velocity distribution on the laminar region of a jet is in agreement with Bickley's theoretical result.

(2) The flow pattern of a jet at a reduced disturbance level is classified according to the slit Reynolds number $R_s$ ($= 2U_0 h/\nu$) as follows:

$12 < R_s < 20 \sim 30$. The jet is entirely laminar or periodic fluctuations exist in a very small region.

$20 \sim 30 < R_s < 40 \sim 60$. Periodic fluctuations are found in a wide region of the jet. They die out without developing into irregular fluctuations.

$40 \sim 60 < R_s$. Irregular fluctuations are observed downstream of the region of periodic fluctuations.

(3) The frequency of periodic fluctuation is roughly proportional to the square of the jet velocity.

(4) No turbulent burst is observed in the transition region.

(5) The validity of linearized stability theory is confirmed by the experiment when the Reynolds number is not too small. For the local Reynolds number $R_b$ ($= U_0 b/\nu$) smaller than 10, the existing theory seems to be unrealistic because it neglects the streamwise variation of the flow field.

(6) The existence of a critical Reynolds number is not verified experimentally.

The authors appreciate the stimulating discussions held throughout the whole course of the investigation with members of the Boundary-Layer Research Group in Japan, which is directed by Prof. Itiro Tani. Thanks are extended to Mr Y. Onda who helped to carry out the experiment.

## REFERENCES

ANDRADE, E. N. DA C. 1939 *Proc. Phys. Soc.* **51**, 784.

BICKLEY, W. G. 1937 *Phil. Mag.* (7), **23**, 727.

BROWN, G. B. 1935 *Proc. Phys. Soc.* **47**, 703.

CHANAUD, R. C. & POWELL, A. 1962 *J. Acoust. Soc. Amer.* **7**, 907.

CLENSHAW, C. W. & ELLIOTT, D. 1960 *Quart. J. Mech. Appl. Math.* **13**, 300.

CURLE, N. 1957 *Proc. Roy. Soc.* A, **238**, 489.

HOWARD, L. N. 1958 *J. Math. Phys.* **37**, 283.

KOHLRAUSCH, W. 1881 *Ann. Phys. Chem.* **13**, 545.

KRUGER, F. & SCHMIDTKE, E. 1919 *Ann. Physik*, **60**, 701.

LESSEN, M. & FOX, J. A. 1955 50 *Jahre Grenzschichtforschung*, p. 122. Ed. by H. Görtler & W. Tollmien. Braunschweig.

ROSHKO, A. 1954 *Nat. Adv. Comm. Aero., Wash., Rep.* no. 1191.

SATO, H. 1960 *J. Fluid Mech.* **7**, 53.

SAVIC, P. 1941 *Phil. Mag.* (7), **32**, 245.

TATSUMI, T. & KAKUTANI, T. 1958 *J. Fluid Mech.* **4**, 261.